Desalination and Water Treatment
www.deswater.com

doi:10.5004/dwt.2019.23554

156 (2019) 278–291
July

Biosorption - a case study of hexavalent chromium removal with raw pomegranate peel

Femina Abdul Salam, Anantharaman Narayanan*

Department of Chemical Engineering, National Institute of Technology Tiruchirappalli, Tiruchirappalli-620 015, Tamil Nadu, India, Tel. +91 431 2503103, Fax +91431-2500133, email: naraman@nitt.edu (A. Narayanan)

Received 13 August 2018; Accepted 1 December 2018

ABSTRACT

Biosorptive removal of heavy metals from water is an eco-friendly green technology. In this study, raw pomegranate (Punicagranatum L.) peel (RPP), without any modification or activation, was used as biosorbent for the removal of chromium (Cr(VI)). The influence of operating parameters such as pH, contact time, temperature and concentration of Cr(VI) were studied in batch mode. A maximum removal of 100% was achieved for a Cr(VI) solution of concentration 20 mg/L at an optimum pH and temperature of 2 and 313 K respectively in 3 min. Among the isotherms tested, Langmuir adsorption isotherm has good correlation with experimental data. A maximum Cr(VI) biosorption capacity of 370.4 mg/g was observed at 313K under equilibrium conditions. RPP is also effective in the removal of Cr(VI) at higher concentrations. Among the kinetic models, pseudo-second order kinetic model fits the data well. The thermodynamic study reveals that the endothermic biosorption taking place on RPP is physico-chemical in nature. The biosorption mechanism of RPP with Cr(VI) indicates that intra-particle diffusion is not the only rate limiting step and film diffusion also plays a major role in biosorption.

Keywords: Biosorption; Equilibrium; Green technology; Kinetics; Pomegranate Peel; Thermodynamics

1. Introduction

Chromium (Cr(VI)) and chromium (Cr(III)) find application in chrome plating, dyes, pigments, leather tanning and for preserving wood. Among these industries, tannery effluent discharges excess amount of chromium ion to environment. As per the world health organization, the maximum permissible amount of total chromium in drinking water is 0.05 mg L^{-1}. Cr(III) salts generally serve as essential micronutrient for human being in the glucose metabolism, cholesterol and fat and it is toxic at its higher concentration. Cr(VI) has the tendency to accumulate in the food chains on the human beings and cause severe problems like lung cancer, skin, stomach irritation, liver damage as well as other health problems [1,2]. Therefore, it is necessary to remove the Cr(VI) from the aqueous environment. Precipitation as hydroxides, carbonates or sulfides, ion-exchange, membrane filtration, adsorption using activated carbon and electrochemical methods are the major treatment methods for removing chromium in wastewater [1,2]. Electro-chemical coagulation is another technique which is extensively used in the removal of Cr(VI). Researchers have used different electrodes in their study by electrochemical process for the recovery of chromium. A noble-metal oxide (RuO_2/TiO_2/SnO_2) coated titanium plate as the anode with perforated stainless steel cathodes with in-situ-generated hypochlorite gave a recovery of 50%–60% [3]. Electrochemical coagulation using different combinations of electrodes such as Mg as anode - galvanised Fe as cathode [4], Zn as anode -galvanised Fe as cathode [5] and, aluminium, aluminium alloy, and mild steel as anode and galvanized iron as cathode material [6] have been used. However, these processes require electric power and studies were also tried at lower concentrations. Adsorption is identified to be a low cost and efficient method. The major primary parameters for

*Corresponding author.

Presented at the InDA Conference 2018 (InDACON-2018), 20-21 April 2018, Tiruchirappalli, India

biosorption of heavy metal ions are valency, concentration and ionic nature of compound in the solution and binding groups of sorbent material. Further, the removal mechanism depends on size and concentration of the sorbate molecule in solution, its affinity to sorbent, diffusion coefficient of the sorbate in bulk phase, and pore size distribution of the sorbent [7]. So, the efficiency of the biosorption process depends on the physicochemical properties and sorption capacity of sorbent.

It has been observed that bio-sorbents possess various functional groups which are responsible for binding the contaminant and hence they are identified to be low-cost adsorbent material for the removal of heavy metals from aqueous media. In this regard, agro residues are found to be natural biomass material for the adsorption process. Walnut shell powder [8], avocado kernel seeds, juniperusprocera sawdust and papaya peels [9], prosopisjuliflora [10], waste plant biomass [11] cow hooves [12] marine red alga *Pterocladiacapillacea* [13] soy hull biomass [14], orange peel powder [15] etc. have been extensively used for the removal of Cr. The main idea of utilizing the biosorbent is to make the adsorption process more green and also efficient. However, sufficient ecofriendly biosorbents are yet to be explored for the adsorption of heavy metals.

Pomegranate (*Punicagranatum L*) contains (i) bioactive compounds like ellagitannins, proanthocyanidin compounds, phenolics and flavonoids [16] (ii) minerals like potassium, nitrogen, calcium, phosphorus, magnesium, and sodium [17], and complex polysaccharides. It encompasses both positive and negative groups such as hydroxyl, amine and carboxylic groups which can easily bind metal ions [18]. Thus, it can possibly bind versatile group of anionic and cationic metal ions. The bioactive compounds such as phenolic and anthocyanins derivatives have the property of good free radical scavenging properties which also enhances the chelating property with metal ions. Polyphenols can also undergo redox reactions by which they can easily donate hydrogen to reducing agents [19]. All the above-mentioned properties led to the selection of RPP as metal chelating agent for the biosorption of hexavalent chromium especially at higher initial concentrations of chromium. The main objectives of the study are:

- Removal of Cr(VI) from synthetic solution using an ecofriendly bio-sorbent, RPP, under batch adsorption mode.
- Evaluation of Cr(VI) biosorption efficiency using four different adsorption isotherms such as the Langmuir, Freundlich, Temkin and Dubinin-Rasdushkevich isotherms.
- The order of biosorption kinetics is also studied to find the rate and mechanism of adsorption.

2. Materials and methods

2.1. Chemicals

Potassium dichromate ($K_2Cr_2O_7$), HCl, NaOH, H_2SO_4 and 1,5-diphenylcarbazide (DPC) procured from Merck Company were used in the entire study. All the chemicals used were of analytical grade.

2.2. Sorbent preparation

The pomegranate peel, a juice industry waste, collected from National Institute of Technology (NIT), Tiruchirappalli campus, was washed thoroughly with tap water to remove dust and dirt and subsequently washed thrice with double distilled water (DDW). The sample was then dried in sunlight for two days and then in hot air oven at 313K for 24 h. It was then crushed manually with a hammer, and subsequently sieved and separated to different size fractions using sieve shaker and stored in airtight containers. Particles retained on 125 µm mesh were used for the study.

2.3. Sorbent characterization

Prepared RPP material was characterised using BET apparatus (Micromeritics, Gemini-V2), FTIR (Perkin Elmer 4000) unit, XRD unit (Rigaku Ultima III), SEM (VEGA3, TESCAN (CZECH REPUBLIC)) and EDAX unit (BRUKER nano, GmbH, D-12489 (Germany).

2.4. Hexavalent chromium detection

Colorimetry is preferred for the detection of Cr(VI). To obtain calibration curve, the stock solution of 1000 mg/L was prepared by dissolving 2.835 g of dichromate in 1 L DDW. Different concentrations, namely, 1, 2, 3, 4 and 5 mg/L were prepared from the above solution by serial dilution. 5 ml each of this was added to a mixture of 1 ml of DPC (0.25 g dissolved in 50 ml acetone) and 1 ml of 2 N H_2SO_4. The solution was then mixed well and kept for 5–10 min to develop a pink color. The mechanism for complex formation is such that the hydrolysis of Cr(VI) at pH above 6 produces CrO_4^{2-}, which reduces immediately to Cr(III) in acidic medium and simultaneous oxidation of DPC to 1,5-diphenylcarbazone, generates a complex of pink colour. This was measured using UV-vis spectrophotometer at 540 nm. The reaction mechanism with Cr(VI) and reagent DPC is given as follows [20]:

$$2\,CrO_4^{2-} + 3\,H_4L + 8\,H^+ \rightarrow Cr(III)\,(HL)_2^+ + Cr^{3+} + H_2L + 8\,H_2O \quad (a)$$

where H_4L and H_2L are diphenylcarbazide and diphenylcarbazone respectively.

2.5. Determination of Point of Zero Charge (pH_{PZC}) and optimum pH

The point of zero charge (pH_{PZC}) is an important parameter to find whether the biomaterial can adsorb anionic or cationic material. Above pH_{PZC}, the charge on the surface of the biosorbent is negative and it can adsorb cations and below which it can adsorb anions. For determining pH_{PZC} point of the biomaterial, 50 ml each 0.01 M NaCl solution were taken in six different conical flasks with pH ranging from 2–12. It was then stirred in a rotary shaker with 0.5 g of raw material for 24 h. The pH of the solution was adjusted with 0.1 M HCl and 0.1 M NaOH. The final pH of the solution was then measured. The graph was plotted with ΔpH against initial pH.

Optimum pH is crucial as it affects not only the surface charges but also the ionic forms of the solute in water [21]. Cr(VI) exists in its ionic form, primarily as salts of chromic acid (H_2CrO_4), hydrogen chromate ion ($HCrO_4^-$) and chromate ion (CrO_4^{2-}). H_2CrO_4 predominates at a pH less than 1.0, $HCrO_4^-$ predominates at a pH between 1.0 and 6.0, and CrO_4^{2-} predominates at a pH above 6.0. The dichromate ion ($Cr_2O_7^{2-}$), a dimer of $HCrO_4^-$ minus a water molecule forms when the concentration of chromium exceeds approximately 1 g/L [22]. From the Eh-Ph diagram of Cr(VI) [22] and speciation diagram [20,22] it was noted that chromium ions were present as Cr^{3+}in highly acidic medium.

The determination of optimum pH involves the preparation of solutions with concentrations 20, 50 and 100 mg/L from the stock solution. 100 ml each of 20 mg/L solution was taken in seven conical flasks with 0.05 g of RPP in each of the conical flasks. The solutions were equilibrated for 150 min (equilibrium time) in an incubator shaker at 150 rpm. The pH of the solutions were varied from 1 to 7 using 0.1 N NaOH and 0.1 N HCl. The samples were filtered using 0.45 µm, 47 mm MF-Millipore filter paper. The concentration of residual Cr(VI) was determined. The experiments were repeated with Cr(VI) solutions of concentrations 50 and 100 mg/L. Higher values of pH were not preferred as it leads to the precipitation of Cr(VI).

2.6. Batch adsorption study

The effect of initial Cr(VI) concentration and contact time of the solution for biosorption of Cr(VI) on RPP was studied at 303K. The Cr(VI) solutions of concentrations 20, 50, 100, 250 and 500 mg/L were prepared from stock solution. 100 ml solution from each concentration was taken in each of the 250 ml conical flask with 0.05 g RPP. The solutions were then agitated in an incubator shaker at 150 rpm. Samples were drawn till 150 min, at time intervals of 3, 6, 10, 30, 60, 120 and 150 min for analysing the residual chromium. The experiments were conducted at an optimum pH of 2. For calculating the thermodynamic parameters, free energy (ΔG°), enthalpy (ΔH°), and entropy (ΔS°), the same procedure was repeated at temperatures of 313 and 323K for Cr(VI) solutions at concentrations of 50, 100 and 250 mg/L.

2.6.1. Biosorption equilibrium

The equilibrium sorption capacity (q_e) and percentage removal of Cr(VI) are calculated from Eqs. (1) and (2).

$$\text{Equilibrium sorption capacity}, q_e = \frac{(C_0 - C_e)V}{M}(mg/g) \quad (1)$$

$$\%\ \text{Removal} = \left(\frac{C_0 - C_e}{C_0}\right) \times 100 \quad (2)$$

$$\text{Distribution coefficient},\ k_d = \frac{(C_0 - C_e)V}{C_e M} \quad (3)$$

where C_0 and C_e, are the initial and equilibrium concentrations of Cr(VI) in mg/L, V is the volume of solution in litre (L) and M is the mass (g) of RPP added to the solution. q_e is the amount of sorbate adsorbed on one gram of sorbent at equilibrium (mg/g) and k_d is the Distribution coefficient (L/g).

2.6.2. Biosorption isotherm

The applicability of adsorption isotherms, the Langmuir [23,24], Temkin [23] and Dubinin-Rasdushkevich (DR) isotherms [24–28] will be verified based on the correlation coefficients, R^2 and normalized standard deviation, Δq_e [29].

Langmuir equation: $$\frac{C_e}{q_e} = \frac{1}{b \cdot \Theta} + \frac{C_e}{\Theta} \quad (4)$$

Separation factor: $$R_L = \frac{1}{1 + bC_0} \quad (4.1)$$

Freundlich equation: $$\ln q_e = \ln K + \frac{1}{n} C_e \quad (5)$$

Temkin equation: $$q_e = a + b \ln C_e \quad (6)$$

$$a = \frac{RT}{B_t} \ln(A) \quad (6.1)$$

$$b = \frac{RT}{B_t} \quad (6.2)$$

DR isotherm equation: $$\ln q_e = \ln q_m - k_{DR} \varepsilon^2 \quad (7)$$

$$\varepsilon = RT \ln\left(1 + \left(\frac{1}{C_e}\right)\right) \quad (7.2)$$

where C_0 and C_e, are the initial and equilibrium concentrations of Cr(VI) in mg/L, V is the volume of solution in litre (L) and M is the mass (g) of RPP added to the solution. q_e is the amount of sorbate adsorbed on one gram of sorbent at equilibrium (mg/g), Θ the constant in Langmuir equation constant is in (mg/g), R_L the separation factor, K a constant in Langmuir equation, the constants of Temkin equation B_t is in L/mg, and A is in mg/g, the constants of DR equation q_m is in (mg/g) E is in (kJ/mol).

2.6.3. Biosorption kinetics

Optimized conditions like rate-limiting step are essential for the design of biosorption systems [29]. These can be studied with kinetic models. Biosorption capacity, 'q_t', as a function of time 't', will be determined using Eq. (8) [30].

$$\text{Adsorption capacity at time (t) is given by}, q_t = \frac{(C_0 - C_t)V}{M}(\text{mg/g}) \quad (8)$$

Pseudo first order kinetic model equation is given by [29,31],

$$\ln(q_e - q_t) = \ln q_e - k_1 t \quad (9)$$

However, if the errors in q_e predicted and q_e observed is more, modified Pseudo-first order kinetic model will

be tested. The Eq. (10) gives modified Pseudo first order kinetic model [31].

$$\frac{q_t}{q_e} + \ln\left(q_e - q_t\right) = \ln q_e - k_{1m} t \tag{10}$$

Pseudo-second order kinetic model is given in [6,29,31,32,33] by Eq. (11)

$$\frac{t}{q_t} = \frac{1}{k_2 q_e^2} + \frac{1}{q_e} t \tag{11}$$

Elovich kinetic model is given by Eq. (12)

$$q_t = \frac{1}{\beta}\ln(\alpha\beta) + \frac{1}{\beta}\ln t \tag{12}$$

$$\%\Delta q_t = 100\frac{\sqrt{\Sigma\left(\frac{q_t \exp - q_e cal}{q_t \exp}\right)^2}}{n-1} \tag{13}$$

where q_e and q_t are the amount of sorbate adsorbed on sorbent at equilibrium and at time 't' respectively in mg/g. k_1 and k_2 are the first order (1/min) and second order reaction rate equilibrium constant (g/mg·min) respectively [31]. k_{1m} is the modified first order reaction rate constant [31]. α and β are the initial adsorption rate (mg/g min) and the desorption constant (g/mg) based on the availability of adsorption surface and activation energy for chemisorption [31]. 1/β value shows the number of sites available for adsorption whereas the value of $\frac{1}{\beta}\ln(\alpha\beta)$ indicates the adsorption quantity. Elovich model does not predict any particular mechanism but it is useful for predicting the adsorption on highly heterogeneous adsorbents [32].

2.6.4. Biosorption thermodynamics

Thermodynamic parameters, free energy (ΔG°), enthalpy (ΔH°), and entropy (ΔS°), were calculated using the Eq. (14)–(16) [29,30,34].

$$\Delta G° = -RT\ lnK_c \tag{14}$$

$$K_c = \frac{C_{Ae}}{C_e} \tag{14.1}$$

$$\ln K_c = -\frac{\Delta H°}{RT} + \frac{\Delta S°}{R} \tag{15}$$

$$\ln k_2 = lnA - \frac{E_a}{RT} \tag{16}$$

where R is the universal gas constant (8.314 J/mol·K), T is the absolute temperature in Kelvin, K_c is the equilibrium constant and C_{Ae} and C_e in mg/L, are the equilibrium concentrations of solute in solid and liquid phase respectively. The slope and intercept of the plot $ln\frac{C_{Ae}}{C_e}$ vs. 1/T provides ΔH° and ΔS° values.

2.6.5. Biosorption mechanism

Identification of rate controlling step is very important to understand the type of mechanism associated with the adsorption phenomena. Important mechanisms followed in adsorption process are (a) Film diffusion – movement of solute molecules from the bulk to the surface of adsorbent (b) intraparticle diffusion or pore diffusion - the movement of solute from the surface of sorbent to the interior parts (c) adsorption of solute on the interior surface of the pores of the sorbent [31,35]. Usually, film and pore diffusions are basic steps that control adsorption rate in batch systems and in continuous system film diffusion is the rate controlling step [36].

2.6.5.1. Macro and micropore diffusion or intraparticle diffusion or Weber and Morris model

The mechanism of adsorption of Cr(VI) on RPP was interpreted by the intraparticle diffusion model given in Eq. (17) [23,29,37]

$$q_t = k_{ip} t^{1/2} + C_1 \tag{17}$$

where q_t is the amount of Cr(VI) adsorbed and k_{ip} is the intraparticle diffusion rate constant (mg/g $min^{\frac{1}{2}}$). The intercept C_1 was obtained from the plot of q_t vs. $t^{1/2}$. The role of boundary layer thickness is reflected in the value of C_1. The larger the values of intercept, the greater is the boundary layer effect [23,37,38]. If the plot is linear and passes through the origin, intraparticle diffusion becomes the sole rate-limiting step [31]. If the linear plot is not passing through the origin, then intraparticle diffusion is not the only rate limiting step [29]. Totally three processes are controlling the rate of adsorption, but only one is the rate limiting at any particular time or stage of adsorption. Since the slope of the linear portion indicates the rate of the process, lower value of slope corresponds to slower process [7].

2.6.5.2. Boyd model

Boyd kinetic model indicates whether the film diffusion or the particle diffusion is the rate-limiting step based on the linearity of plot between B_t and time [31]. If the plot is linear and passes through the origin, then particle diffusion becomes the rate limiting step; otherwise film diffusion is the rate limiting step. The model equations are presented in Eqs. (18)–(21).

$$F = 1 - \frac{6}{\pi^2}\exp\left(-B_t\right) \tag{18}$$

$$F = \frac{q_t}{q_e} \tag{19}$$

where q_t and q_e are same as mentioned earlier. F represents the fraction of solute adsorbed at any time "t" and B_t is a mathematical function of F. After taking natural logarithm, Eq. (18) can be rearranged to

$$B_t = -0.4977 - \ln\left(1 - F\right) \tag{20}$$

$$B_t = \frac{\pi^2 D_i}{r^2} \quad (21)$$

B_t calculated from Eq. (20) is used for finding the effective diffusion coefficient, D_i (m^2/g) of the solute in the sorbent phase with the help of Eq. (21). '*r*' is the radius of the adsorbent particles.

3. Results and discussions

3.1. Characterization of raw pomegranate peel

The surface area of the material was found to be 5.04 m^2/g, using BET apparatus. The predicted value was found to match with the reported value for Raw Pomegranate Peel (RPP) [29]. The surface morphology of RPP before and after biosorption of Cr(VI) obtained from SEM is shown in Figs. 1a and 1b respectively. From Fig. 1a it is clear that the surface texture of RPP resembles like scattered structure with coarse particles. From Fig. 1 it is clear that morphology of RPP changed after the biosorption of Cr(VI). In the case of Cr(VI) biosorbed RPP, the morphology is in the form of clumps with brighter illumination. It is due to the existence of metal Cr(VI) ions which produce glossy appearance under morphology analysis. Moreover, the surface morphology of the biosorbent became comparatively smoother after the biosorption of Cr(VI) and the pores and channels are occupied by Cr(VI) ions giving a comparatively smother surface [39,40]. As can be seen in Fig. 1(b), the aggregation of particles reveals that Cr(VI) biosorption on RPP is over the biosorbent surface. This phenomenon is due to redox reaction between active sites on the surface of biosorbent and Cr(VI) ions.

The presence of alkali and alkaline earth metals in biomaterials are illustrated in an earlier study [18]. The EDAX spectrum of RPP shown in Fig. 2 indicates the presence of alkaline metal Potassium and alkaline earth metal Calcium along with C, O, Cu and Cl. Traces of other elements like Zn, Mn, Fe and Se were also observed. Immediate neutralization of the oxyanion, $HCrO_4^-$ of Cr(VI), with these protonated sites might be possible [29].

FTIR spectra of the sorbent in Fig. 3, show the variation of bonds before and after biosorption of Cr(VI). Major changes could be seen in wavenumber between 1750 cm^{-1} and 500 cm^{-1}. The change in peaks near wavenumber 1000–1100 cm^{-1} is due to the changes in counter ions associated with carboxylate and hydroxylate anions. This enlightens the predominant role of the functional groups for the removal of metal ion [18]. The presence of C-Br and C-Cl bonds near 564.04 cm^{-1} and 873.6 cm^{-1} were also reported earlier in the case of biomaterial [41]. This indicates, that the groups present in this region play major role in biosorption.

The strong peak at wavenumber 1010 cm^{-1} has been reduced with the formation of one small peak at wavenumber 1146 cm^{-1}. More bond formations were also observed between the wave numbers 1400–1100 cm^{-1} and 1750–1600 cm^{-1}. Changes in O-H stretching vibrations at 3723–3000 cm^{-1} region shows the inter and intra-molecular hydrogen bonding of alcohols, phenols and carboxylic acids groups in biosorption [42]. New bonds formed at 1357, 1313, 1146, 582 and 510 cm^{-1} confirm the formation of new compounds with the biomaterial.

3.2. Effect of pH on Cr(VI) removal

From Fig. 4a, the point of zero charge (pH_{pzc}) of the biomaterial RPP was found to be 3.8. The value indicated that the material can adsorb negatively charged ions for pH < 3.8 and positively charged ions at pH > 3.8 Fig. 4b shows the effect of pH on the percentage removal of chromium at 303K for 150 min. For low concentrations of 20 mg/L, the removal was almost 100% up to a pH of 6 and then varied at pH 7. But in the case of higher concentration (100 mg/L), the percentage removal decreases sharply from 100 to 60% at a pH range of 2–3 and then continuously reduced to 44% at a pH of 7. Thus, the optimum pH was predicted to be 2 for all the experiments, which was used for further analysis (kinetics, isothermal, thermodynamic and mechanism were studied for 250 and 500 mg/L also). The decrease in biosorption with an increase in pH of solution, was mainly due

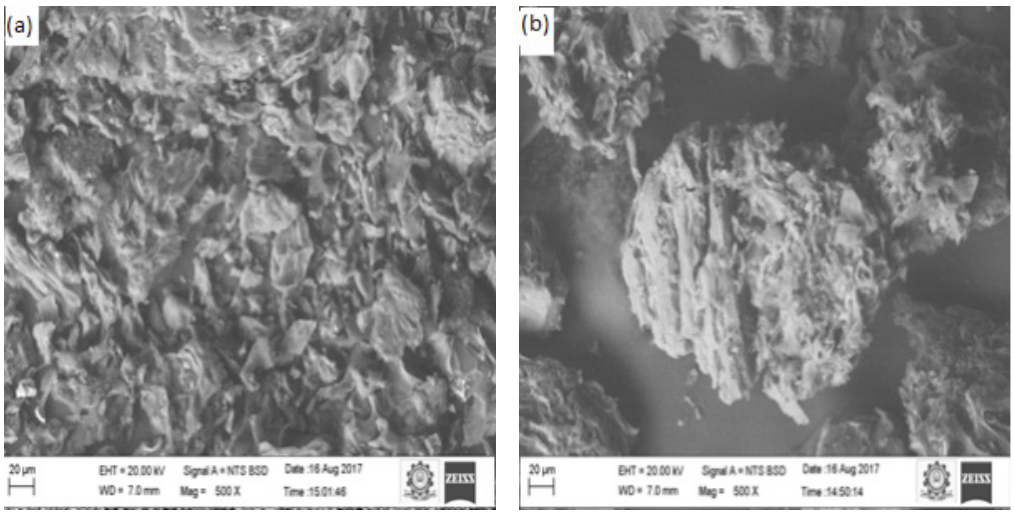

Fig. 1. SEM images of pomegranate peel (A) before and (B) after chromium sorption on RPP at 303K, pH 2 and 50 mg/L concentration.

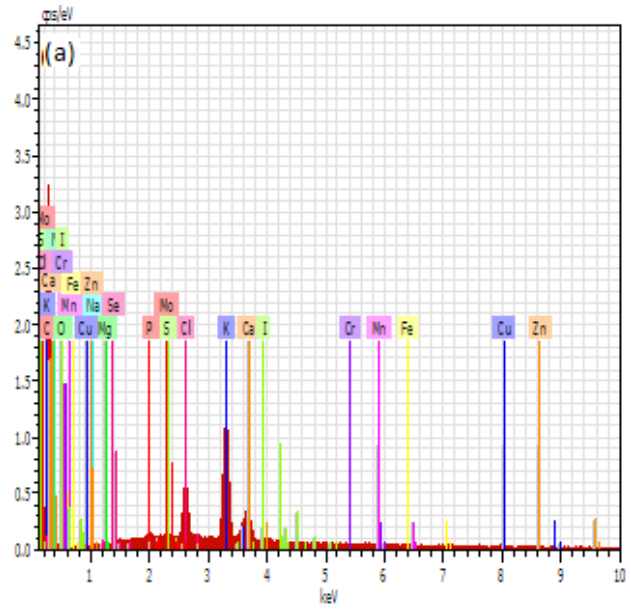

Fig. 2. EDAX spectra of pomegranate peel.

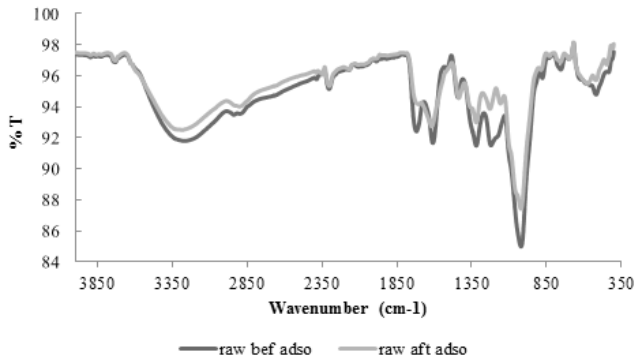

Fig. 3. FTIR spectra of RPP before and after sorption of Cr(VI) from 50 mg/L Cr(VI) solution.

to the decrease in electrostatic force of attraction between the sorbent and the sorbate ions [21].

Possible mechanisms for the reduction of Cr(VI) to Cr(III), for the removal of Cr(VI) involves the steps as follows:

(i) Reduction of Cr(VI) to Cr(III) by surface electron donor groups of sorbent and then reduced Cr(III) forms complexes with adsorbent or remain in solution. (ii) biosorption coupled reduction of Cr(VI) to Cr(III) on the sorbent sites. Three steps involved in this mechanism are (a) binding of the anionic $HCrO_4^-$ of Cr(VI) to the protonated sites on the adsorbent, (b) reduction of adsorbed Cr(VI) to Cr(III) by adjacent electron donor groups (CO, O-CH_3) on the adsorbed site of sorbent, (c) release of surface reduced Cr(III) into the solution due to electronic repulsion between protonated groups on sorbent surface and surface bound Cr(III). Chromium reduction reactions occurring in acidic medium reported earlier are [21].

$$HCrO_4^- + 7H^+ + 3e^- \leftrightarrow Cr^{3+} + 4H_2O \quad (a)$$

$$CrO_4^{2-} + 8H^+ + 3e^- \leftrightarrow Cr^{3+} + 4H_2O \quad (b)$$

$$Cr_2O_7^{2-} + 14H^+ + 6e^- \leftrightarrow 2Cr^{3+} + 7H_2O \quad (c)$$

The most abundant surface functional group, amphoteric and extremely reactive, hydroxyl groups present in pomegranate peel is responsible for surface complexation reaction [21]. Under acidic conditions, the sorbent surface becomes more protonated, which favours the sorption of anionic form of chromium [21]. This is the first step in the complexation reaction followed by second step which involves, the acidic functional groups present in the surface which in turn enhances the biosorption of formed Cr(III) and suppresses adsorption of Cr(VI) [22]. The possible hydrolysis reactions occurring for Cr(III) are given in literature [22].

$$Cr^{3+} + H_2O \leftrightarrow [Cr(OH)]^{2+} + H^+ \quad (d)$$

$$[Cr(OH)]^{2+} + HA \leftrightarrow ([Cr(OH)]^{2+} - A^-) + H^+ \quad (e)$$

where A represents an adsorption site on acidic surface of the pomegranate peel.

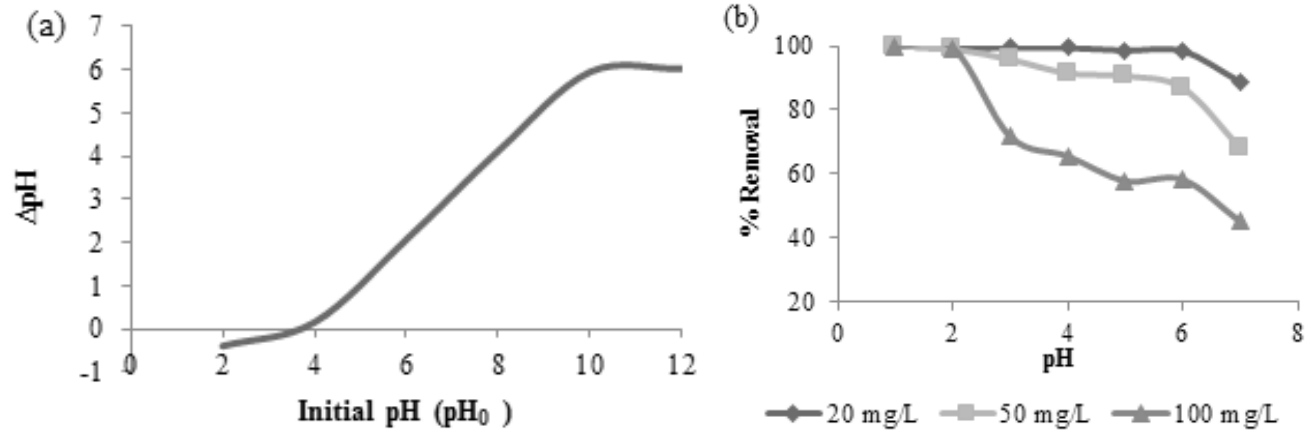

Fig. 4. (a) Point of zero charge (pH_{PZC}) of the adsorbent, (b) Effect of pH and initial concentration of Cr(VI) on percentage removal at 303K for 150 min.

The overall reaction for Cr(III) adsorption is given by,

$$Cr^{3+} + H_2O \leftrightarrow ([Cr(OH)]^{2+} - A^-) + 2H^+ \quad (f)$$

Another favourable reaction at low pH expected on the surface of the adsorbent is the neutralisation of negative charges by excess H^+ ions. The neutralisation improves the diffusion of anionic form of Cr(VI), ($HCrO_4^-$), and its subsequent sorption [22]. From the FTIR spectra,the identified functional groups R-COOH, R-OH, R- NH_2, hydroxyl and unprotonated aminogroups act as coordination and electrostatic interaction sites for Cr(III). Suggested Cr(III) sorption mechanisms reported in literature [22] are as follows.

$$Cr^{3+} + R\text{-}OH \leftrightarrow R\text{-}O\text{-}Cr^{2+} + H^+ \quad (g)$$

$$Cr^{3+} + R\text{-}NH_2 \leftrightarrow Cr(R\text{-}NH_2)^{2+} + H^+ \quad (h)$$

The tannin compounds are found to occur naturally in RPP. The adsorptive removal of Cr(VI) on condensed tannin gels derived from natural materials containing polyhydroxyphenyl groups were explained by earlier investigators. The mechanism suggested was useful for the complete removal of chromium by "zero emission oriented process" [43]. The mechanisms were (i) esterification of chromate with tannin molecules (ii) reduction of Cr(VI) to Cr(III) (iii) carboxyl group formation by tannin oxidation (iv) ion exchange of reduced Cr(III) with carboxyl and hydroxyl groups. A large amount of proton consumption follows Cr(VI) reduction and neutralisation of acidic Cr(VI) solution at proper initial pH. The carboxyl group formed during the reduction of Cr(VI) to Cr(III) and tannin oxidation creates more ion exchange sites for the sorption of Cr(III) formed.

Atomic absorption spectroscopy (AAS) analysis was also carried out for checking the presence of total chromium in the remaining solution. It was not detectable for solutions with 10 and 20 mg/L as initial concentration of chromium. However, a negligible amount was observed with a Cr(VI) solution of initial concentration 50 mg/L and 0.98 mg/L with a Cr(VI) solution initial concentration 100 mg/L indicating that hexavalent chromium was present. This also confirmed that for lower concentrations this biomaterial is suitable for 100% removal of total chromium.

3.3. Biosorption equilibrium

The equilibrium sorption capacity (q_e) and percentage removal of Cr(VI) were calculated from Eqs. (1) and (2) and presented in Figs. 5a and 5b.

The effect of initial concentration of Cr(VI) and contact time on biosorption capacity and percentage removal are presented in Figs. 5a and Fig. 5b at pH 2 and 303K respectively. As the initial concentration of the solute and the contact time of the biosorbent and sorbate increases, the biosorption capacity increases. Initially, the biosorption rate was found to be very high (at all concentrations, more than 70% of maximum capacity is achieved within 10 min) due to large number of available active sites and then it reduces and reaches a stable condition because of the non-availability of active sites. The biosorption capacity increases from 41.44 to 382.07 mg/g as the concentration increases from 20 to 500 mg/L at the equilibrium time of 150 min and at a temperature of 303K. For all the concentrations, biosorption capacity shows significant variations upto 90 min and after that it remains almost stable. At a temperature of 303K, the percentage removal was 99.22 for an initial concentration of 20 mg/L while the removal was 84.06, 68.84, 53.15, and 38.91 at the 30th minute for an initial concentration of 50, 100, 250 and 500 mg/L respectively. The respective biosorption capacities were 41.11, 70.27, 153.47, 279.483 and 352.989 mg/g. The extension of time to equilibrium leads to100% removal of chromium from the solution of concentration 20 mg/L at 303K.

The distribution coefficient, k_d calculated using Eq. (3), describes that when the adsorbent surface is alike, the binding ability of an adsorbent surface to the adsorbate will not change with adsorbent dosage, otherwise it will change with dosage [44]. The calculated values of k_d are presented in Table 1. The k_d values were found to change with temperature and sorbent dosage. An increase in temperature leads to an increase in pore size on the sorbent surface which enhances the diffusion of metal ions through the pores to the internal regions. As temperature increases, the contact between sorbate molecules and sorbent surface also increases.

3.4. Biosorption isotherm

The applicability of adsorption isotherms, the Langmuir [23,24], Freundlich [23], Temkin [23] and Dubinin-Rasdushkevich (DR) isotherms [24–28] were verified as per Eqs. (4)

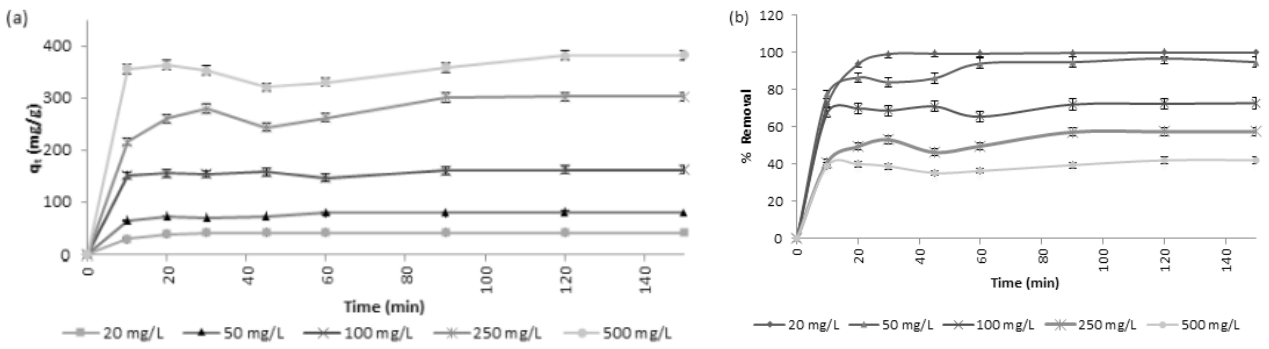

Fig. 5. (a) Effect of initial concentration of Cr(VI) and time of contact on sorption capacity at pH 2 and 303K, (b) Effect of initial concentration of Cr(VI) and time of contact on % removal at pH 2 and 303K.

Table 1
Distribution coefficient k_d at different temperatures, pH 2 and an adsorbent dosage 0.5 g/L

Temperature K	k_d values (L/g) at different concentration				Average k_d values (L/g)
	50 (mg/L)	100 (mg/L)	250 (mg/L)	500 (mg/L)	
303	60.73	11.412	2.700	1.455	19.074
313	437.2	24.842	2.679	1.227	116.487
323	527.5	19.667	2.889	1.462	137.879

Table 2
Isotherm parameters for Chromium removal on pomegranate peel

Temp (K)	Langmuir			Freundlich			Temkin			D-R		
	R^2	Θ (mg/g)	B (L/mg)	R^2	k	$1/n$	R^2	a	b	R^2	q_m (mg/g)	E (kJ/mol)
303	0.986	384.6	0.084	0.949	56.08	0.36	0.972	42.55	56.88	0.120	165.9	1.17
							B_t = 44.29 L/mg, A = 2.113 mg/g					
313	0.992	370.4	0.144	0.732	83.88	0.26	0.898	103.7	42.29	0.093	167.2	4.11
							B_t = 61.53 L/mg, A = 11.623 mg/g					
323	0.981	400	0.103	0.750	84.09	0.27	0.876	105.8	45.71	0.106	172.2	4.46
							B_t = 58.743 L/mg, A = 10.13 mg/g					

to (7.2) based on the correlation coefficients, R^2 and normalized standard deviation, Δq_e [29]. Details are presented in Table 2 and in Fig. 6.

The R^2 values of the isotherm models (Figs. 6a–d) show the fitness of data in the order of Langmuir > Temkin > Freundlich > DR. From Langmuir isotherm, Θ , the maximum monolayer adsorption capacity (mg/g), and '*b*', a constant related to the energy of adsorption (L/mg), under the experimental conditions were estimated as cited in literature [45]. The isotherm parameters are summarised in Table 2. In Freundlich adsorption isotherm, "*n*" indicates the bond energy between the metal ion and the sorbent and *K* represents the bond strength. '1/*n*' value for all the three temperature conditions are between 0 and 1, which indicates good biosorption. The positive value of energy of biosorption B_t (L/mg) by Temkin isotherm predicted an endothermic process. According to Dubinin-Radushkevich (DR) Isotherm the adsorption is physisorption in nature as the mean free energy of adsorption or apparent energy change (*E*) in kJ/mol, defined as the energy change that occurs when one mole of sorbate ion is transferred from the bulk solution to the surface of the sorbent, is less than 8 kJ/mol [46].

The dimensionless separation factor, R_L, gives the feasibility and applicability of the process based on the initial concentration of the solution. If $R_L > 1$ biosorption is unfavourable, $R_L = 1$ it is linear, $0 < R_L < 1$ biosorption is favourable and $R_L = 0$ the biosorption is irreversible [29,41]. In the present study, 'R_L' values (Table 3) were less than one (average of the five concentrations) and the decrease in values with increase in concentration gives an indication of more favourable sorption at higher concentrations of Cr(VI). R_L values at 313K were very less compared to other temperatures, which mean that the temperature favourable for biosorption is 313K.

3.5. Biosorption kinetics

The kinetic models were tested using Eqs. (8)–(13) described earlier. This is essential for the design of biosorption systems. Details are presented in Fig. 7 and Table 4.

For kinetic model validation (Figs. 7a–d and Table 4), R^2 values and normalised standard deviation, Δq_t (%), calculated from Eq. (13) were used. The value of R^2 indicates the model fitness and applicability [29]. In Eq. (13), '*n*' represents the number of data points; q_{exp} and q_{cal} in mg/g are the experimental and calculated biosorption capacity values. The lower value of Δq_t for pseudo-second order model at 303K indicates a good agreement between experimental and calculated data. Compared to the values obtained from pseudo second order model, the difference between q_e, experimental and q_e, calculated are high for other models. The decrease in model coefficient with increase in initial feed concentration of Cr(VI) was due to the greater competition for the active sorbent sites and due to the decrease in electrostatic interaction [29]. All these reveal that the rate limiting step of Cr(VI) biosorption on RPP follows pseudo-second order model with chemisorption involving covalent bonds or ionic bonds by which sharing or exchange of electrons between sorbate molecules and surface functional groups of sorbent occurred [25,27]. As per the data reported earlier [31,42] the adsorption capacity of Persimmon tannin and Acroptilon repens flower powder are 5.27 mol/kg and 5.72 mg/g respectively. In the present study, RPP showed a

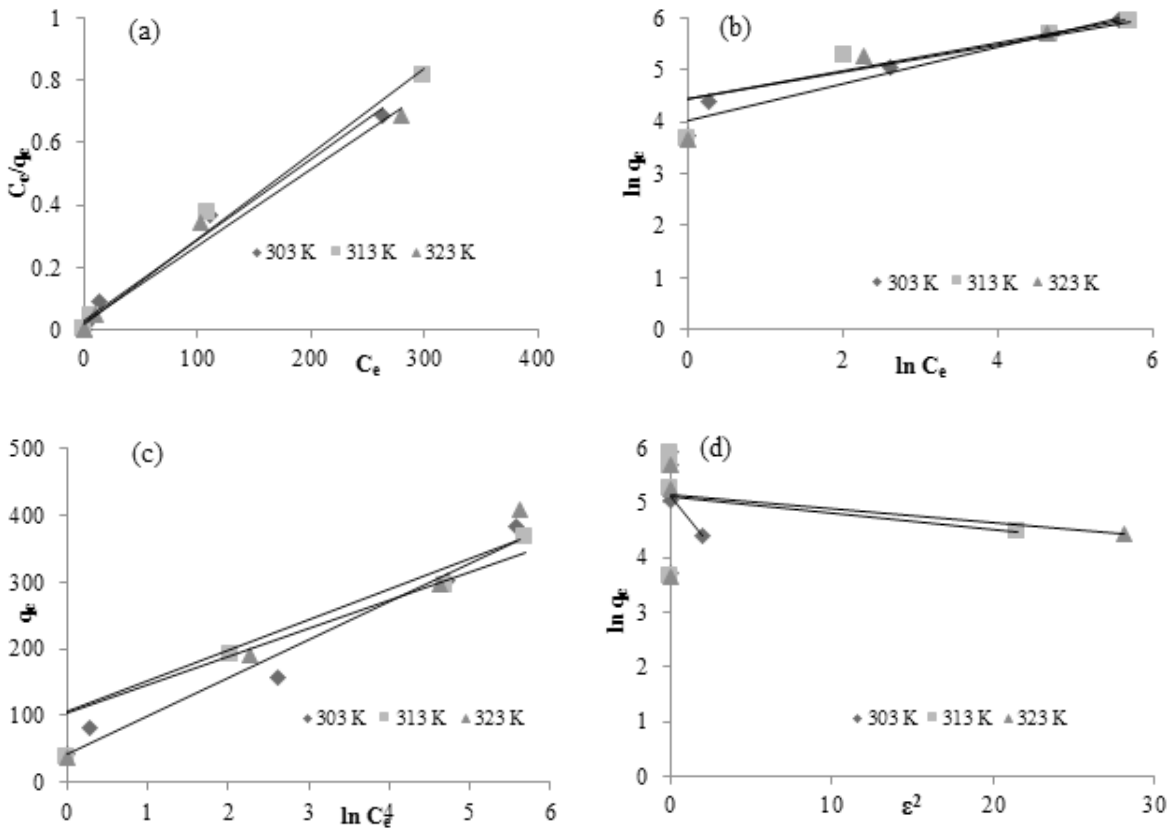

Fig. 6. Isotherm plots of (a) Langmuir (b) Freundlich (c) Temkin and (d) D-R for the removal of Cr(VI) at room temperature of 303K.

Table 3
Separation factor for Langmuir isotherm

Temperature (K)	R_L values at different initial chromium concentration (mg/L)					Average R_L-values (mg/L)
	20	50	100	250	500	
303	0.365	0.222	0.114	0.043	0.026	0.154
313	0.267	0.135	0.063	0.026	0.014	0.101
323	0.338	0.185	0.085	0.037	0.0196	0.133

maximum biosorption capacity of 370.4 mg/g at 313K and it is higher than the earlier reported values. It displays that the RPP would be an effective biosorbent material for Cr sorption. RPP particle can also be tested for biosorption of other anionic metal ions.

3.6. Biosorption thermodynamics

Thermodynamic parameters, free energy (ΔG°), enthalpy (ΔH°), and entropy (ΔS°), were calculated using Eqs. (14)–(16) [29,30,34].

The minimum energy required to start the biosorption process, activation energy of adsorption E_a (kJ/mol), can be calculated from Arrhenius equation Eq. (16), where k_2 is pseudo second-order kinetic model rate constant (g/mg·min) and A is the Arrhenius factor [29]. The value of ($-E_a/R$) was estimated from the plot of ln k_2 vs. 1/T.

The negative values of free energy of biosorption, ΔG°, calculated from Eq. (14) shows the spontaneous nature of the process and high negative values with an increase of temperature shows favourable nature of the process [34]. The decrease in numerical values with a negative sign in the direction of increase in concentration indicates that biosorption is favourable at higher concentrations. All the ΔG° values obtained were less than 20 kJ/mol, and this confirms that the biosorption process is physisorption [29,47,48,49].

Table 5 presents the thermodynamic parameters for the removal of Cr(VI) using RPP. 72% removal of Cr(VI) is obtained from a solution of 20 mg/L within 10 min at 303K, which enhanced to 100% within 3 min at 313K. A similar increase in removal was noticed for concentrations of 50 mg/L and 100 mg/L, but not much at higher concentrations of 250 and 500 mg/L. The positive values of ΔH° indicate the endothermic nature of the process [29,34]. This

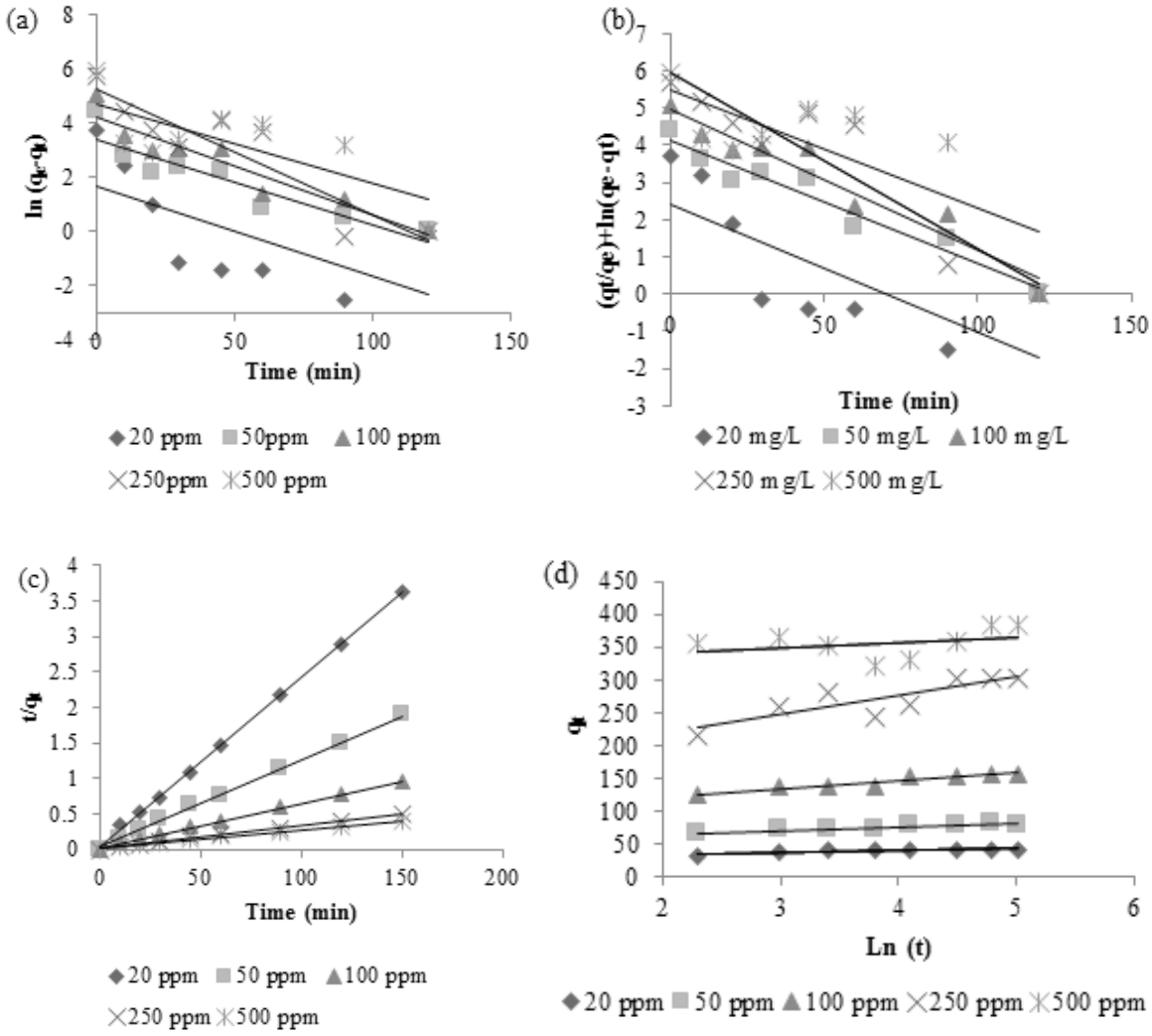

Fig. 7. Kinetic plots of (a) Pseudo first order (b) Modified Pseudo first order (c) Pseudo second order and (d) Elovich model for the removal of Cr(VI) at room temperature of 303K and pH 2.

behaviour might be due to the increase of sorbate molecules diffusing through the external film and internal pores of the sorbent [29,50,51]. Increase in biosorption with the rise in temperature may be attributed to diffusion controlled process due to the increased number of biosorption sites generated due to the breakage of some internal bonds [34]. The positive values of ΔS° suggest an increase in the degree of freedom at the solid-liquid interface and the randomness at the sorbent surface [52]. This may be due to the release of (i) aqua molecules and (ii) hydrogen ions for Cr(III) or hydroxyl ion for Cr(VI) when the sorbate species is being sorbed by the biosorbent. This supports the ion-exchange adsorption mechanism of sorbate at their respective pH values [53]. As the concentration of the feed increases, the ΔS° value decreases, which means that the randomness has got reduced and the system has become stable. The variation in the percentage removal of Cr(VI) with time at different temperatures (303, 313 and 323K) and at a pH of 2 is plotted in Fig. 8b and the maximum percentage removal was observed at a temperature of 313K.

3.7. Biosorption mechanism

The type mechanism associated with biosorption phenomena can be identified through the rate controlling step.

3.7.1. Macro and micropore diffusion or intraparticle diffusion or Weber and Morris model

The mechanism of biosorption of Cr(VI) on RPP can be interpreted by the intraparticle diffusion model given in Eq. (17) presented earlier [23,29,37]. The details are presented in Fig. 9 and Table 6.

The dual nature of biosorption curve shown in Fig. 9a is due to the changes in mass transfer rate between initial and final stages of biosorption [32]. In the initial phase, from the slope of the graph it is clear, that the rate constant increases with increase in concentration and the plot is passing through the origin and bulk diffusion becomes the rate

Table 4
Kinetic parameters for chromium removal on pomegranate peel

Model	Kinetic parameters	Initial concentration of chromium (mg/L)				
		20	50	100	250	500
Pseudo first order	q_{eexp} (mg/g)	41.438	80.937	156.704	302.100	382.068
	k_1 (min^{-1})	0.033	0.032	0.036	0.046	0.030
	q_{ecal} (mg/g)	5.117	29.424	68.979	188.859	112.967
	R^2	0.405	0.848	0.622	0.829	0.548
	Δq_t (%)	30.735	21.383	18.345	10.791	24.104
Modified pseudo first order	q_{eexp} (mg/g)	41.438	80.937	156.704	302.100	382.068
	k_{1m} (min^{-1})	0.034	0.033	0.038	0.047	0.032
	q_{ecal} (mg/g)	10.951	61.295	141.982	378.418	246.559
	R^2	0.558	0.945	0.930	0.852	0.560
	Δq_t (%)	25.485	6.564	2.963	15.751	10.877
Pseudo second order	q_{eexp} (mg/g)	41.438	80.937	156.704	302.100	382.068
	k_2 (min^{-1})	0.018	0.005	0.002	0.001	0.001
	q_{ecal} (mg/g)	41.841	81.301	158.730	312.500	384.615
	R^2	1.000	0.999	0.998	0.994	0.994
	Δq_t (%)	5.109	4.397	5.124	7.621	3.745
Elovich model	q_{eexp} (mg/g)	41.438	80.937	156.704	302.100	382.068
	α (mg/g min)	8997	55298	21127	7387	9 E+18
	β (g/mg)	0.297	0.174	0.078	0.035	0.128
	q_{ecal} = 1/β (mg/g)	3.366	5.731	12.821	28.790	7.828
	Δq_t (%)	32.315	32.630	32.184	31.554	34.575
	R^2	0.610	0.872	0.890	0.732	0.110

Table 5
Thermodynamic parameters for Cr(VI) removal on pomegranate peel

Concentration (mg/L)	ΔH° (J mol^{-1})	ΔS° (J mol^{-1} K^{-1})	ΔG° (J mol^{-1})			*E* (J mol^{-1})	A
			303 K	313 K	323 K		
50	88660.5	323.29	–8598.5	–13927	–14971.2	46554.2	485046.5
100	22574.2	90.3	–4387.1	–6556.2	–6138.3	5566.63	0.01493
250	2730.2	11.4	–756.3	–789.12	–988.31	296078.2	3.7E+47

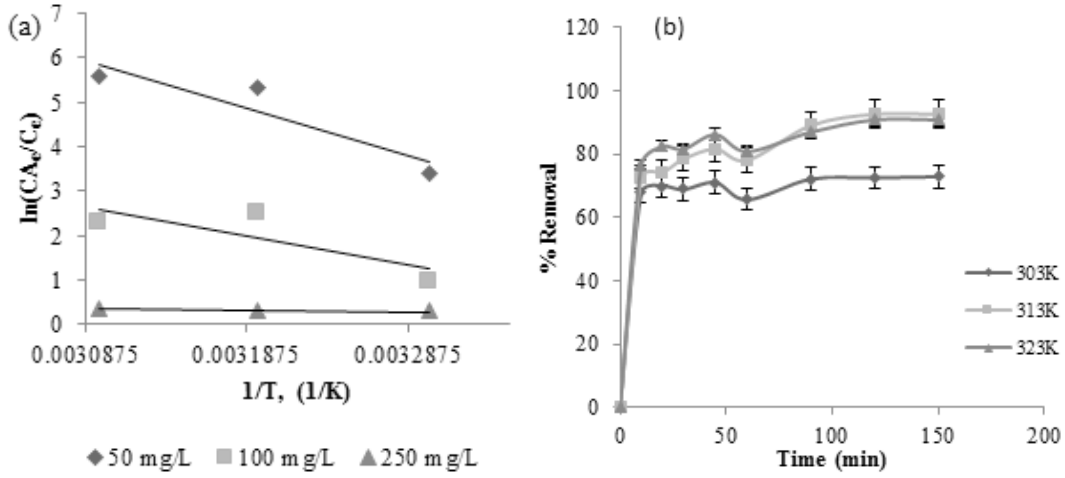

Fig. 8. (a) Thermodynamic parameter ΔH° and ΔS° estimation plot for Cr(VI) removal with three different initial feed concentration and 0.5 g/L dosage of adsorbent at 303, 313 and 323K (b) Removal of Cr(VI) at 303, 313 and 323K for 100 mg/L feed concentration.

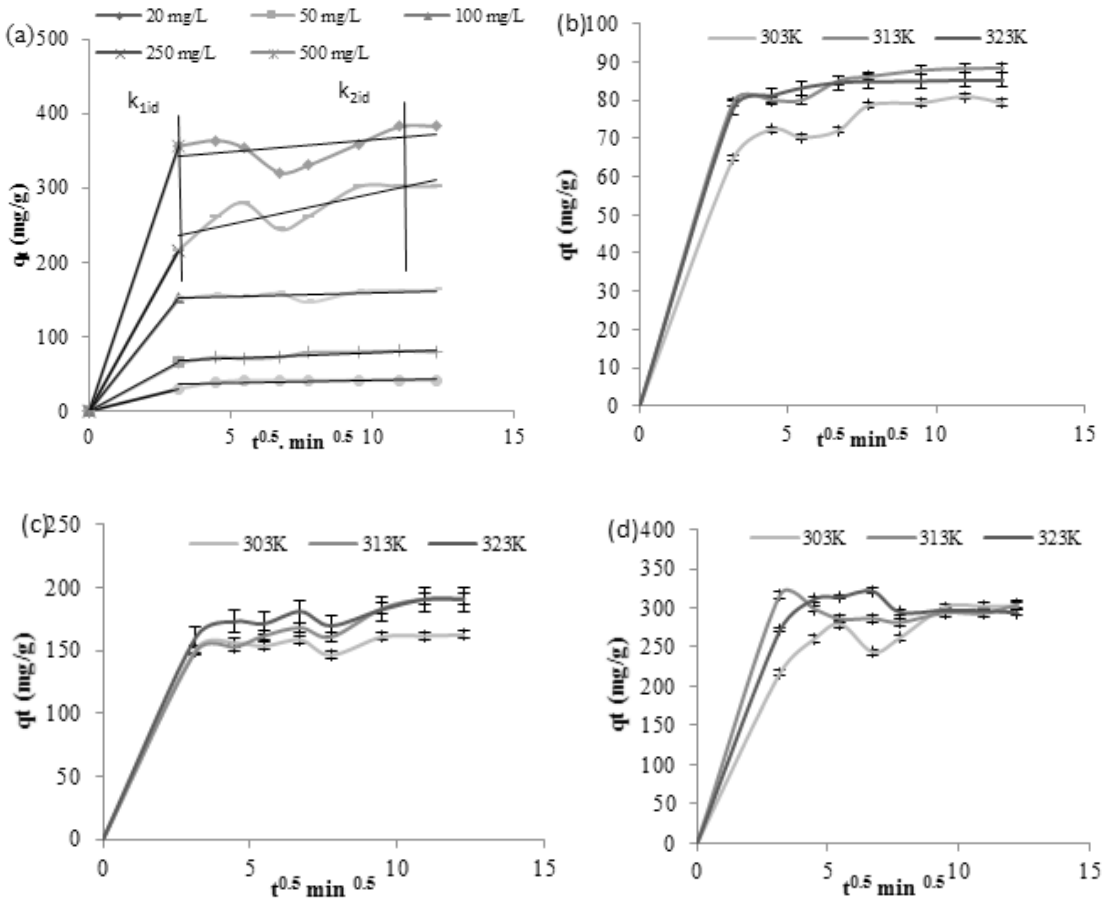

Fig. 9. Macro and micropore diffusion plot (a) for different initial concentration of Cr(VI) at 303K. (b), (c) and (d) are the variation of biosorption capacity at 303, 313 and 323K for 50,100 and 250 mg/L concentrations of Cr(VI) respectively at 2 pH.

Table 6
Macro and micropore diffusion data

Model parameters	Concentration (mg/L)				
	20	50	100	250	500
$k_{1id\ (mg/g.\ min^{0.5})}$	9.451	20.486	47.766	68.456	112.65
$k_{2id\ (mg/g.\ min^{0.5})}$	0.829	1.610	1.1435	8.244	3.190
C_1	6.00E-15	1.00E-14	0.00E+00	0.00E+00	0.00E+00
C_2	33.313	62.583	147.590	208.810	331.890
R_1^2	1	1	1	1	1
R_2^2	0.437	0.812	0.412	0.708	0.214

controlling step. The diffusion of Cr(VI) ions through the solution to the external surface of the sorbent happens here. In the second phase, gradual sorption stage, diffusion of the solute into mesopores occurs. The regression line intercepts, deviate from the origin with increase in concentration. The rate of removal of solute from the bulk depends on the size of the sorbate molecule, the concentration of the sorbate, diffusion coefficient of sorbate in the bulk of the solution and the pore size distribution of the sorbent [7]. The third portion of the plot is linear which suggests biosorption into the micropores of the sorbent. This makes the sense that intraparticle diffusion in micropores is the rate-limiting step in the biosorption process. Macro and micropore diffusion data calculated are tabulated in Table 6.

Figs. 9b–d indicate that as the temperature increases the biosorption takes place faster for all concentrations. The mobility of the molecules towards the sorbate increases and the film diffusion stage becomes more steeper, (i.e.)the biosorption rate constant increases with increase in concentration and the second stage is attained little earlier at 313 and 323K than at 303K. However, not much variation was observed in biosorption rate between 313 and 323K.

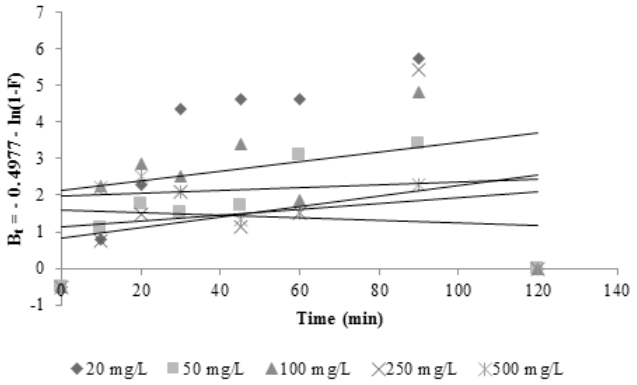

Fig. 10. Boyd plot for the biosorption of Cr(VI) pomegranate peel at 30°C.

3.7.2. Boyd model

To identify whether the film diffusion or the particle diffusion is the rate-limiting step Boyd model was tested using the model equations presented in Eqs. (18)–(21). The results are presented in Fig. 10.

It is observed from Fig. 10 that all the plots are showing dual behaviour and none of them are linear and they are also not passing through the origin. This indicates that pore diffusion or internal diffusion is not the sole step for controlling the rate of biosorption, but film diffusion is also the controlling step. After the 30th min, all the plots were changing their trend from initial slope to horizontal, due to the difference in mass transfer between two stages. The average B_t values and the effective diffusion coefficients calculated from Eq. (20) and Eq. (21) are 3.135, 1.726, 1.668, 1.704, 1.633 and 1.242×10^{-09}, 6.8×10^{-10}, 6.61×10^{-10}, 6.7×10^{-10}, 6.47×10^{-10} m^2/s respectively for the initial concentrations of 20, 50, 100, 250 and 500 mg/L.

4. Conclusion

The equilibrium, kinetic, thermodynamic and biosorption mechanism study with raw pomegranate peel was conducted for the biosorptive removal of Cr(VI). It was observed that 0.5 g/L of 125 µm size RPP can remove 100% Cr(VI) from 20 mg/L Cr(VI) solution within 3 min at 313K. Langmuir isotherm gave a good fit with a higher R^2 value of 0.9918 and an biosorption capacity of 370.4 mg/g at 313K. Isotherm and kinetic study suggests that the system follows physicochemical biosorption with pseudo second order kinetics respectively and the thermodynamic study suggested favourable, spontaneous, endothermic biosorption in the direction of an increase in solute concentration. Biosorption mechanism and the intraparticle diffusion model suggest that more than one mechanism controls the rate-limiting step and this has been supported by Boyd model. Atomic absorption spectroscopy (AAS) analysis confirms that the presence of total chromium in the remaining solution is negligible. All the above observations suggest that RPP of 125 µm size is a very good eco-friendly biosorbent for the removal of Chromium Cr(VI) even with a very low dosage of 0.05 g in 100 ml.

References

[1] F. Fu, Q. Wang, Removal of heavy metal ions from wastewaters: A review, J. Environ. Manage., 92 (2011) 407–418.
[2] A.G.D. Prasad, M.A. Abdullah, Biosorption of Cr(VI) from synthetic wastewater using the fruit shell of gulmohar (delonix regia): Application to electroplating wastewater, Bio Resources, 5 (2010) 838–853.
[3] G. Sozhan, S. Mohan, S. Vasudevan, R. Balaji, S. Pushpavanam, Recovery of chromium from the solid residue by in-situ-generated hypochlorite, Ind. Eng. Chem. Res., 45 (2006) 7743–7747.
[4] S. Vasudevan, J. Lakshmi, R. Vanathi, Electrochemical coagulation for chromium removal: process optimization, kinetics, isotherms and sludge characterization, Clean, 381 (2010) 9–16.
[5] S. Vasudevan, J. Lakshmi, Studies relating to an electrochemically assisted coagulation for the removal of chromium from water using zinc anode, Water Sci. Technol.: Water Supply., 11 (2011) 142–150.
[6] S. Vasudevan, J. Lakshmi, G. Sozhan, Studies on the Al–Zn–In-alloy as anode material for the removal of chromium from drinking water in electrocoagulation process, Desalination, 275 (2011) 260–268.
[7] W.H. Cheung, Y.S. Szeto, G. McKay, Intraparticle diffusion processes during acid dye adsorption onto chitosan, Bioresour. Technol., 98 (2007) 2897–2904.
[8] A.M. Farhan, N.M. Salem, A.H. Al-Dujaili, A.M. Awwad, Biosorption studies of Cr(VI) ions from electroplating wastewater by walnut shell powder, Am. J. Environ. Eng., 2 (2012) 188–195.
[9] E. Mekonnen, M. Yitbarek, T.R. Soreta, Kinetic and thermodynamic studies of the adsorption of Cr (VI) onto some selected local adsorbents, South Afr. J. Chem., 68 (2015) 45–52.
[10] M. Kumar, R. Tamilarasan, Kinetics, equilibrium data and modeling studies for the sorption of chromium by Prosopis juliflora bark carbon, Arab. J. Chem., 10 (2013) S1567–S1577.
[11] A. Mishra, A. Dubey, S. Shinghal, Biosorption of chromium(VI) from aqueous solutions using waste plant biomass, Int. J. Environ. Sci. Technol., 12 (2015) 1415–1426.
[12] I. Osasona, A.O. Adebayo, O.O. Ajayi, Adsorptive removal of chromium (VI) from aqueous solution using cow hooves, J. Sci. Res. Reports., 2 (2013) 288–303.
[13] A. El Nemr, A. El-Sikaily, A. Khaled, O. Abdelwahab, Removal of toxic chromium from aqueous solution, wastewater and saline water by marine red alga Pterocladiacapillacea and its activated carbon, Arab. J. Chem., 8 (2015) 105–117.
[14] P.S. Blanes, M.E. Bordoni, J.C. González, S.I. García, A.M. Atria, L.F. Sala, S.E. Bellu, Application of soy hull biomass in removal of Cr(VI) from contaminated waters. Kinetic, thermodynamic and continuous sorption studies, J. Environ. Chem. Eng., 4 (2016) 516–526.
[15] N.M. Rane, R.S Sapkal, Chromium(VI) removal by using orange peel powder in batch adsorption, Int. J. of Chem. Sci. Appl., 5 (2014) 22–29.
[16] Y. Li, C. Guo, J. Yang, J. Wei, J. Xu, S. Cheng, Evaluation of antioxidant properties of pomegranate peel extract in comparison with pomegranate pulp extract, Food Chem., 96 (2006) 254–260.
[17] S.H. Mirdehghan, M. Rahemi, Seasonal changes of mineral nutrients and phenolics in pomegranate (Punicagranatum L.) fruit, Sci. Hortic. (Amsterdam)., 111 (2007) 120–127.
[18] R. Lakshmipathy, N.C. Sarada, Application of watermelon rind as sorbent for removal of nickel and cobalt from aqueous solution, Int. J. Miner. Process., 122 (2013) 63–65.
[19] M. Viuda-Martos, J. Fernandez-Lopez, J.A. Perez-Alvarez, Pomegranate and its many functional components as related to human health: a review, Compr. Rev. Food Sci. Food Saf., 9 (2010) 635–654.
[20] X. DIONE, Determination of Cr(VI) in water, wastewater and solid waste extracts, Tech. Note 26LPN34398--011M7/96, Dionex Corp., 1996.

[21] E. Pehlivan, H. Kahraman, E. Pehlivan, Sorption equilibrium of Cr(VI) ions on oak wood charcoal (Carbo Ligni) and charcoal ash as low-cost adsorbents, Fuel Process. Technol., 92 (2011) 65–70.
[22] D. Mohan, C.U. Pittman, Activated carbons and low cost adsorbents for remediation of tri- and hexavalent chromium from water, J. Hazard. Mater., 137 (2006) 762–811 .
[23] E.S.Z. El-Ashtoukhy, N.K. Amin, O. Abdelwahab, Removal of lead (II) and copper (II) from aqueous solution using pomegranate peel as a new adsorbent, Desalination, 223 (2008) 162–173.
[24] M. Khitous, Z. Salem, D. Halliche, Effect of interlayer anions on chromium removal using Mg-Al layered double hydroxides: Kinetic, equilibrium and thermodynamic studies, Chinese J. Chem. Eng., 24 (2016) 433–445.
[25] A. Maiti, S. D. Gupta, J.K. Basu, S. De, Adsorption of arsenite using natural laterite as adsorbent, Sep. Purif. Technol., 55 (2007) 350–359.
[26] J. Romero-González, J.R. Peralta-Videa, E. Rodriíguez, S.L. Ramirez, J.L. Gardea-Torresdey, Determination of thermodynamic parameters of Cr(VI) adsorption from aqueous solution onto Agave lechuguilla biomass, J. Chem. Thermodyn., 37 (2005) 343–347.
[27] J. Romero-González, J.R. Peralta-Videa, E. Rodríguez, M. Delgado, J.L. Gardea-Torresdey, Potential of Agave lechuguilla biomass for Cr(III) removal from aqueous solutions: Thermodynamic studies, Bioresour. Technol., 97 (2006) 178–182.
[28] A. El Nemr, A. Khaled, O. Abdelwahab, A. El-Sikaily, Treatment of wastewater containing toxic chromium using new activated carbon developed from date palm seed, J. Hazard. Mater., 152 (2008) 263–275.
[29] M.A. Ahmad, N.A. Ahmad Puad, O.S. Bello, Kinetic, equilibrium and thermodynamic studies of synthetic dye removal using pomegranate peel activated carbon prepared by microwave-induced KOH activation, Water Resour. Ind., 6 (2014) 18–35.
[30] C. Hua, R. Zhang, F. Bai, P. Lu, X. Liang, Removal of chromium (VI) from aqueous solutions using quaternized chitosan microspheres, Chinese J. Chem. Eng., 25 (2017) 153–158.
[31] M.T. Ghaneian, A. Bhatnagar, M.H. Ehrampoush, M. Amrollahi, B. Jamshidi, M. Dehvari, M. Taghavi, Biosorption of hexavalent chromium from aqueous solution onto pomegranate seeds: kinetic modeling studies, Int. J. Environ. Sci. Technol., 14 (2017) 331–340.
[32] P.S. Kumar, S. Ramalingam, S.D. Kirupha, A. Murugesan, T. Vidhyadevi, S. Sivanesan, Adsorption behavior of nickel (II) onto cashew nut shell: Equilibrium, thermodynamics, kinetics, mechanism and process design, Chem. Eng. J., 167 (2011) 122–131.
[33] A. Pandiarajan, R. Kamaraj, S. Vasudevan, OPAC (orange peel activated carbon) derived from waste orange peel for the adsorption of chlorophenoxyacetic acid herbicides from water: Adsorption isotherm , kinetic modelling and thermodynamic studies, Bioresour. Technol., 261 (2018) 329–341.
[34] J. Acharya, J.N. Sahu, B.K. Sahoo, C.R. Mohanty, B.C. Meikap, Removal of chromium(VI) from wastewater by activated carbon developed from Tamarind wood activated with zinc chloride, Chem. Eng. J., 150 (2009) 25–39.
[35] J.N. Sahu, J. Acharya, B.C. Meikap, Optimization of production conditions for activated carbons from Tamarind wood by zinc chloride using response surface methodology, Bioresour. Technol., 101 (2010) 1974–1982.
[36] S. Goswami, U.C. Ghosh, Studies on adsorption behaviour of Cr (VI) onto synthetic hydrous stannic oxide, Water SA., 31 (2005) 597–602.
[37] P.S. Kumar, S. Ramalingam, V. Sathyaselvabala, S.D. Kirupha, S. Sivanesan, Removal of copper (II) ions from aqueous solution by adsorption using cashew nut shell, Desalination, 266 (2011) 63–71.
[38] N. Kannan, M.M. Sundaram, Kinetics and mechanism of removal of methylene blue by adsorption on various carbon - a comparative study, Dye. Pigm., 51 (2001) 25–40.
[39] A. Ali, K. Saeed, F. Mabood, Removal of chromium (VI) from aqueous medium using chemically modified banana peels as efficient low-cost adsorbent, Alexandria Eng. J., 55 (2016) 2933–2942 .
[40] M.A. Mahmoud, M.M. El-Halwany, Adsorption of cadmium onto orange peels: isotherms, kinetics, and thermodynamics, J. Chromatogr. Sep. Tech., 05(5) (2014). doi:10.4172/2157-7064.1000238.
[41] N.F. Fahim, B.N. Barsoum, A.E. Eid, M.S. Khalil, Removal of chromium (III) from tannery wastewater using activated carbon from sugar industrial waste, J. Hazard. Mater., 136 (2006) 303–309.
[42] K. Huang, Y. Xiu, H. Zhu, Removal of hexavalent chromium from aqueous solution by crosslinked mangosteen peel biosorbent, Int. J. Environ. Sci. Technol., 12 (2015) 2485–2492.
[43] Y. Nakano, K. Takeshita, T. Tsutsumi, Adsorption mechanism of hexavalent chromium by redox within condensed-tannin gel, Water Res., 35 (2001) 496–500.
[44] X. Yu, S. Tong, M. Ge, J. Zuo, Removal of fluoride from drinking water by cellulose@hydroxyapatite nanocomposites, Carbohydr. Polym., 92 (2013) 269–275.
[45] K. Mohanty, M. Jha, B.C. Meikap, M.N. Biswas, Removal of chromium (VI) from dilute aqueous solutions by activated carbon developed from Terminalia arjuna nuts activated with zinc chloride, Chem. Eng. Sci., 60 (2005) 3049–3059.
[46] S.K. Maji, A. Pal, T. Pal, A. Adak, Adsorption thermodynamics of arsenic on laterite soil, J. Surf. Sci. Technol., 23 (2007) 161–176.
[47] O.S. Bello, T.A. Fatona, F.S. Falaye, O.M. Osuolale, Adsorption of eosin dye from aqueous solution using groundnut hull – based activated carbon : kinetic, equilibrium, and thermodynamic studies, Environ. Eng. Sci., 29 (2012) 186–194.
[48] N.S. Nasri, M. Jibril, M.A.A. Zaini, R. Mohsin, H.U. Dadum, A.M. Musa, Synthesis and characterization of green porous carbons with large surface area by two step chemical activation with KOH, J. Teknol. Sci. Eng., 67 (2014) 25–28.
[49] S.S. Batool, Z. Imran, S. Hassan, K. Rasool, M. Ahmad, M.A. Rafiq, Enhanced adsorptive removal of toxic dyes using SiO_2 nanofibers, Solid State Sci., 55 (2016) 13–20.
[50] M.J. Ahmed, Application of agricultural based activated carbons by microwave and conventional activations for basic dye adsorption: Review, J. Environ. Chem. Eng., 4 (2016) 89–99.
[51] M.J. Ahmed, Preparation of activated carbons from date stones by chemical activation method using $FeCl_3$ and $ZnCl_2$ as activating agents, J. Eng., 17 (2011) 1007–1022.
[52] M.H. Baek, C.O. Ijagbemi, O. Se-Jin, D.-S. Kim, Removal of Malachite Green from aqueous solution using degreased coffee bean, J. Hazard. Mater., 176 (2010) 820–828.
[53] S. Debnath, U.C. Ghosh, Kinetics, isotherm and thermodynamics for Cr(III) and Cr(VI) adsorption from aqueous solutions by crystalline hydrous titanium oxide, J. Chem. Thermodyn., 40 (2008) 67–77.